MOLECULAR AND CELLULAR BIOLOGY, July 1995, p. 3805–3812 Vol. 15, No. 7
0270-7306/95/$04.00+0

Constitutive Phosphorylation of eps8 in Tumor Cell Lines: Relevance to Malignant Transformation

BRONA MATOSKOVA,[1] WILLIAM T. WONG,[2] ANNA ELISABETTA SALCINI,[3] PIER GIUSEPPE PELICCI,[3,4] AND PIER PAOLO DI FIORE[2,5]*

Laboratory of Cellular Development and Oncology, National Institute of Dental Research,[1] and Laboratory of Cellular and Molecular Biology, National Cancer Institute,[2] Bethesda, Maryland 20892, and Istituto di Medicina Interna e Scienze Oncologiche, Policlinico Monteluce, Perugia,[3] Istituto di Patologia Medica, University of Parma, Parma,[4] and Istituto di Microbiologia, Facoltá di Medicina e Chirurgia, Bari,[5] Italy

Received 24 February 1995/Returned for modification 29 March 1995/Accepted 17 April 1995

eps8, a recently identified tyrosine kinase substrate, has been shown to augment epidermal growth factor (EGF) responsiveness, implicating it in EGF receptor (EGFR)-mediated mitogenic signaling. We investigated the status of eps8 phosphorylation in normal and transformed cells and the role of eps8 in transformation. In NIH 3T3 cells overexpressing EGFR (NIH-EGFR), eps8 becomes rapidly phosphorylated upon EGF stimulation. At receptor-saturating doses of EGF, ~30% of the eps8 pool is tyrosine phosphorylated. Under physiological conditions of activation (i.e., at low receptor occupancy), corresponding to the 50% effective dose of EGF for mitogenesis, ~3 to 4% of the eps8 contains phosphotyrosine. In human tumor cell lines, we detected constitutive tyrosine phosphorylation of eps8, with a stoichiometry (~5%) similar to that associated with potent mitogenic response in NIH-EGFR cells. Overexpression of eps8 was able to transform NIH 3T3 cells under limiting conditions of activation of the EGFR pathway. Concomitant tyrosine phosphorylation of eps8 and shc, but not of rasGAP, phospholipase C-γ, and eps15, was frequently detected in tumor cells. This suggested that eps8 and shc might be part of a pathway which is preferentially selected in some tumors. Cooperation between these two transducers was further indicated by the finding of their in vivo association. This association was, at least in part, dependent on recognition of shc by the SH3 domain of eps8. Our results indicate that eps8 is physiologically part of the EGFR-activated signaling and that its alterations can contribute to the malignant phenotype.

Receptor tyrosine kinases (RTKs) transduce signals for mitogenesis and differentiation through their ability to recruit intracellular signal transducers. This is achieved by binding and/or phosphorylation of intracellular substrates, as well as through the binding of small adapter molecules which, in turn, enable coupling with downstream effector pathways (for reviews, see references 3, 9, 23, and 32 and references therein). Signal transducers possess, in various assortments, several binding-effector regions, including SH2, SH3, and PH domains (references 1, 3, 14, and 31 and references therein). Each of these domains binds to target sequences with variable specificity. Different SH2s, for example, bind to specific phosphotyrosine (pTyr)-containing motifs (34), whereas SH3s recognize proline-rich regions (5, 16, 29, 44). In addition, these target sequences are frequently present on the same transducer molecules together with the binding domains, projecting the existence of an extensive network of intracellular interactions. Even at the initial level of the signaling cascade, that is, tyrosine phosphorylation of substrates by RTKs, our knowledge is far from complete. Two-dimensional analysis of pTyr-containing proteins after growth factor stimulation of intact cells reveals numerous candidate substrates awaiting characterization (30).

Methodologies that allow cloning of these molecules have been developed in several laboratories (10, 13, 15, 20, 24, 33, 34). We have recently described one such strategy and isolated several novel cDNAs (*eps* clones) representing genes encoding substrates for the epidermal growth factor (EGF) receptor (EGFR). One of these genes was designated *eps*8 (11, 43). The product of the *eps*8 gene is a 97-kDa protein ($p97^{eps8}$). In some cell lines, a second component of 68 kDa ($p68^{eps8}$) is also specifically recognized by anti-eps8 antibodies. $p68^{eps8}$ is not the product of a related gene, since all of its tryptic peptides correspond to tryptic peptides of $p97^{eps8}$ (10); it is not clear, however, whether it is the product of an alternatively spliced mRNA or the result of specific proteolysis. The product of the *eps*8 gene associates with and is phosphorylated by the EGFR in NIH 3T3 fibroblasts overexpressing this receptor (NIH-EGFR). Several other RTKs can phosphorylate eps8 as well (11). In addition, the *eps*8 gene product might be involved in the regulation of cell proliferation, since its overexpression in NIH-EGFR or EGFR-overexpressing hematopoietic cells (32D-EGFR) enhances EGF-dependent mitogenic signals (11).

Many questions regarding the role of eps8 in EGFR signaling remain to be answered. It is important to establish whether eps8 is a physiological substrate for EGFR, or whether its phosphorylation is observed only under conditions of receptor overexpression, as achieved in NIH EGFR and 32D-EGFR (11). It is also of interest to determine whether eps8 can be implicated in mitogenic signaling in a setting representative of physiological conditions, for example, under limiting activation of the EGFR pathway. If so, then one could ask whether alterations of eps8 are detectable and play a role in human tumors. Finally, the molecular interactions of eps8 and, ultimately, its biochemical function remain to be elucidated. In the present study, we addressed these questions by quantitative analysis of eps8 tyrosine phosphorylation in established model systems and human tumors, analysis of the transforming po-

* Corresponding author. Mailing address: Laboratory of Cellular and Molecular Biology, National Cancer Institute, National Institutes of Health, Bldg. 37, Room 1D23, Bethesda, MD 20892. Phone: (301) 496-5277. Fax: (301) 496-8479.

tential of eps8, and investigation of interactions with other components of the signaling network.

MATERIALS AND METHODS

Cell biology. NIH 3T3 fibroblasts transfected with eukaryotic expression vectors for EGFR (NIH-EGFR cells) have been previously described (6). They were cultured in Dulbecco's modified Eagle's medium supplemented with 10% (vol/vol) calf serum. The BALB/MK cell line (38) was cultured in low-calcium Dulbecco's modified Eagle's medium supplemented with 10% dialyzed fetal calf serum and 4 ng of EGF per ml as previously described (38). Human tumor cell lines of epithelial and mesodermal derivation were maintained in Dulbecco's modified Eagle's medium supplemented with 10% fetal calf serum. Human tumor cell lines of hematopoietic derivation were propagated in RPMI plus 10% fetal calf serum. Thymidine incorporation studies and transfection of NIH 3T3 cells were conducted as previously reported (6, 7).

Protein studies. Polyclonal antibodies specific for the *eps*8 gene product were generated against a recombinant glutathione *S*-transferase (GST) fusion protein in the pGEX expression vector (Pharmacia) and have been previously described (11). The antibody used in this study was purified from total serum by affinity chromatography with GST-eps8 covalently conjugated to amino-link (Pierce). Detection of pTyr-containing proteins was performed with a commercially available anti-pTyr monoclonal antibody (Upstate Biotechnology). Anti-phospholipase C-γ (anti-PLC-γ), anti-rasGAP, and anti-shc antibodies were also obtained from a commercial source (Upstate Biotechnology and Signal Transduction Laboratories). An anti-p82/ezrin antibody was generated by using purified ezrin as an antigen and was previously described (13). The anti-eps15 antibodies used have also been previously described (12). The anti-GST antibody was generated by immunizing New Zealand rabbits with purified GST recombinantly produced in *Escherichia coli*. The serum was affinity purified by using GST conjugated to amino-link (Pierce). EGFR was detected with either the Ab-1 monoclonal antibody (Oncogene Science) for immunoprecipitation experiments or with E7 antipeptide serum (8) for immunoblotting. When available (eps8 and eps15 experiments), preimmune sera derived from the same rabbits used for immunization were used as controls. In all other cases, preimmune sera from different animals were used as controls.

Immunoprecipitation and immunoblotting experiments were performed as previously described (10–13). Typically, we employed 100 to 200 μg of total cellular proteins for direct immunoblot analysis and 1 to 6 mg of total cellular proteins for immunoprecipitation-immunoblotting experiments. Except when indicated otherwise, treatment with EGF in vivo was performed at a concentration of 17 nM for 5 to 10 min at 37°C after 12 to 24 h of serum starvation. For coimmunoprecipitation experiments, total cellular proteins were obtained under mild lysis conditions in the absence of ionic detergents to preserve protein-protein interactions, as previously described (11).

Calculation of stoichiometry of in vivo phosphorylation. For our experiment (see Fig. 2B), NIH-EGFR cells were serum starved for 16 h and then treated with 17 nM EGF for 5 min at 37°C. Total cellular proteins (1 mg) were then immunoprecipitated with the anti-pTyr antibody, and the immunocomplexes were recovered onto protein G-Sepharose (ipt-1 [see Fig. 2B]). The supernatant (after immunocomplex recovery) was subjected to two additional immunoprecipitations with anti-pTyr antibody, and immunocomplexes were recovered after each immunoprecipitation (ipt-2 and ipt-3 [see Fig. 2B]). The three sequential immunoprecipitations were performed to ensure that all of the pTyr-containing protein was quantitatively immunoprecipitated. The anti-pTyr immunoprecipitates were then analyzed in an immunoblot with the anti-eps8 antibody. The supernatant left after the third immunoprecipitation reaction (see lane S Fig. 2B) was also analyzed in an immunoblot with the anti-eps8 antibody. This supernatant contained non-tyrosine-phosphorylated eps8 molecules, since anti-pTyr immunoprecipitation was quantitative. Only one-fifth of the total supernatant, corresponding to 200 μg of proteins in the initial material, was loaded. On the same blot, 200 μg of total cellular proteins (see lane T Fig. 2B) from the same preparation used for the immunoprecipitation experiments was loaded. The same procedure was followed for the ezrin and PLC-γ stoichiometry determination employing antiezrin and anti-PLC-γ antibodies in the final blot.

Autoradiographic signals were quantitated in a phosphorimager scanner, and all values were corrected by subtracting the machine background determined on an equal surface of the autoradiogram displaying no specific signals. The values obtained in ipt-1, ipt-2, and ipt-3 were then added to calculate the amount of pTyr-containing substrate (eps8, PLC-γ, or ezrin). This value was compared to that obtained for a non-tyrosine-phosphorylated specific substrate (determined in lane S [see Fig. 2B] with multiplication of the value by 5 to take into account differences in loading) or to the value representing the total amount of the specific substrate in the total cellular proteins (determined in lane T [see Fig. 2B] with multiplication of the value by 5 to take in account differences in loading). Stoichiometry of in vivo phosphorylation was then calculated in two different ways, with the formula (ipt × 100)/[ipt + (S × 5)] and the formula (ipt × 100)/(T × 5). Both formulas yielded comparable results, as expected.

In another experiment (see Fig. 3), 5637 cells were serum starved for 24 h and total cell lysates were prepared. The experimental protocol was as described above, with the following exceptions: (i) 5 mg of total cellular proteins was used in the anti-pTyr immunoprecipitations; (ii) 1/50 of the supernatant (S), corresponding to 100 μg of the proteins in the initial material, was loaded; and (iii) 100 μg of total cellular proteins (T) was loaded. Stoichiometry of in vivo phosphorylation was then calculated in two different ways, with the formula (ipt × 100)/[ipt + (S × 50)] and the formula (ipt × 100)/(T × 50). Both formulas yielded comparable results, as expected.

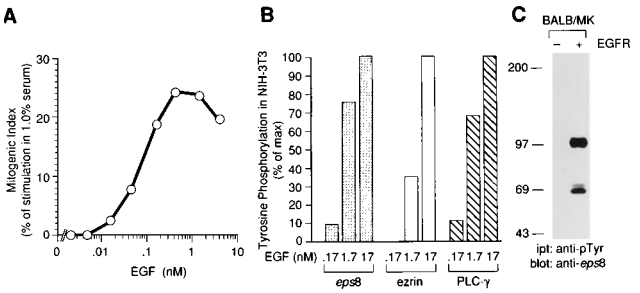

FIG. 1. Tyrosine phosphorylation of *eps*8 gene products in vivo at physiological levels of EGFR activation. (A) NIH-EGFR cells were analyzed for their mitogenic response to increasing concentrations of EGF by [^{3}H]thymidine incorporation. The 50% effective dose for a mitogenic response was 0.1 to 0.2 nM (around 1 ng/ml). (B) Serum-starved NIH-EGFR cells were treated with increasing concentrations of EGF for 10 min at 37°C. Total cellular proteins (2 mg) were immunoprecipitated with the antibodies indicated (anti-eps8, anti-PLC-γ, and antiezrin) and detected in an immunoblot with an anti-pTyr antibody. Quantitation of autoradiographic signals was performed by a phosphorimager scanner, and results are reported as percentages of the maximal phosphorylation obtained at receptor saturation (17 nM) after subtraction of the background signal detected in mock-treated cells. One hundred percent stimulation corresponded to ~20-fold, ~15-fold, and ~15-fold stimulation with respect to untreated cells for eps8, PLC-γ, and ezrin, respectively. (C) Serum- and EGF-starved BALB/MK cells were either mock treated (−) or treated with EGF at 17 nM (+) for 10 min at 37°C. Total cellular proteins (2 mg) were immunoprecipitated with the anti-eps8 antibody and immunoblotted with anti-pTyr. Molecular size markers are indicated in kilodaltons.

EGF binding assay. EGF binding to intact cells was assessed as described previously (6), with ^{125}I-labeled EGF (150 to 200 μCi/μg; New England Nuclear) over a range of concentrations from 0.0017 to 55.6 nM for at least 6 h at 4°C. Assays were performed in triplicate wells, and specificity of binding was determined by parallel experiments in which a 100-fold molar excess of unlabeled EGF was used to eliminate the tracer by competition. The number of receptors per cell and their dissociation constants (K_ds) for EGF were determined from Scatchard plots. Analysis of binding was performed by the LIGAND software (26).

Production of recombinant proteins and in vitro binding studies. The GST-eps8SH3 fusion protein was obtained by amplification, by recombinant PCR, of the appropriate fragment from the eps8 cDNA, followed by cloning in the pGEX expression vector between the *Bam*HI and *Eco*RI sites, in frame with the GST moiety. The SH3 domain of eps8 present in the fusion protein encompasses amino acid residues 532 to 591. The GST–nck-SH3 fusion protein was a kind gift of Octavio Rivero-Lezcano and contains the first SH3 domain of nck (amino acid positions 8 to 68). Purification of the fusion proteins on glutathione-agarose and affinity purification of total cellular proteins on immobilized GST-based fusion proteins have also been described (11).

For far Western (immunoblot) experiments with recombinant GST fusion proteins, blots were blocked in 2% bovine serum albumin (BSA) in TTBS (20 mM Tris-HCl [pH 7.5], 150 mM NaCl, 0.05% Tween 20) for at least 2 h at room temperature and then in reduced glutathione (3 μM; Sigma) in TTBS with 0.5% (wt/vol) BSA for 1 h at room temperature. The latter step substantially reduced the background (data not shown). Blots were then incubated with the appropriate fusion protein (10 nM) in TTBS in the presence of reduced glutathione (3 μM) and BSA (0.5% [wt/vol]) for 1 h at room temperature. After extensive washing in TTBS, blots were detected with the affinity-purified anti-GST antibody as previously described (10–13).

RESULTS

eps8 phosphorylation under physiological conditions of EGF stimulation. We have previously shown that the *eps*8 products are phosphorylated on tyrosine residues by several RTKs (11). By using a model system of NIH-EGFR cells, we initially sought to determine whether eps8 is efficiently phosphorylated under physiological conditions of receptor activation, i.e., at low receptor occupancy. As shown in Fig. 1A, the

TABLE 1. Analysis of ^{125}I-labeled EGF binding properties and eps8 expression levels in NIH-EGFR and BALB/MK cells

Cell line	No. of receptors/cell[a]		K_d (nM)		Relative eps8 level[b]
	High affinity	Low affinity	High affinity	Low affinity	
NIH-EGFR	13,000	350,000	0.1	9.5	1
BALB/MK	15,000		0.07		0.1

[a] ^{125}I-labeled EGF binding was assessed by Scatchard analysis over a range of concentrations from 0.0017 to 55.6 nM in triplicate wells at 4°C as described in Materials and Methods. Specificity of binding was controlled in parallel competition experiments using a 100-fold molar excess of unlabeled EGF. Data were analyzed with the LIGAND software (26).

[b] eps8 expression levels were measured by direct immunoblotting of total cellular proteins, and quantitation was performed by phosphorimaging. Results are expressed relative to the level in NIH-EGFR cells (defined as 1).

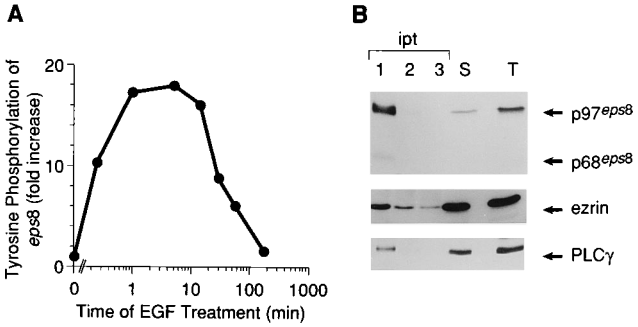

FIG. 2. Time course and stoichiometry of eps8 phosphorylation in vivo. (A) Time course of phosphorylation. NIH-EGFR cells were serum starved for 12 to 16 h and then either mock treated (time zero) or treated with 17 nM EGF at 37°C for the lengths of time indicated. Total cellular proteins (2 mg) were immunoprecipitated with an anti-eps8 antibody and detected in an immunoblot with pTyr antibody. Signal intensities were analyzed in a phosphorimager scanner and expressed as fold increases relative to the signal detected at time zero (assigned an intensity of 1). (B) Stoichiometry of in vivo phosphorylation. NIH-EGFR cells were treated with 17 nM EGF for 5 min at 37°C. Total cellular proteins (1 mg) were then immunoprecipitated three times with the anti-pTyr antibody (ipt-1, ipt-2, and ipt-3), and immunocomplexes were recovered after each immunoprecipitation. Immunoprecipitates were analyzed in an immunoblot with the antibodies indicated (anti-eps8, top panel; antiezrin, middle panel; anti-PLC-γ, bottom panel). The supernatant of the immunoprecipitation reaction (lane S, one-fifth of the total supernatant, corresponding to 200 μg of the initial material) and an aliquot of the total cellular proteins (lane T, 200 μg of proteins) were also analyzed. Autoradiographic signals were quantitated in a phosphorimager scanner. Stoichiometry of in vivo phosphorylation was calculated in two different ways, with the formula (ipt × 100)/[ipt + (supernatant × 5)] and the formula (ipt × 100)/(total × 5). Both formulas yielded comparable results. The positions of specific substrate bands are indicated.

mitogenic dose-response curve for NIH-EGFR cells indicates that half-maximal stimulation was obtained at an EGF concentration of 0.1 to 0.2 nM, whereas maximal stimulation was achieved starting from 1.0 to 2.0 nM. Scatchard plot analysis of ^{125}I-labeled EGF binding to NIH-EGFR cells revealed ~1.3×10^4 high-affinity and ~3.5×10^5 low-affinity binding sites, with K_ds in the range of 10^{-10} to 10^{-8} M, respectively (Table 1). Thus, at the mitogenic 50% effective dose of EGF, only a few thousand receptors would be occupied. At this dose (1 ng/ml, ~0.17 nM), however, eps8 tyrosine phosphorylation was readily detectable and was around 10% of the maximal stimulation obtained with receptor-saturating doses (Fig. 1B). The magnitude of this effect was comparable to or greater than that observed for two established EGFR substrates, PLC-γ and ezrin (Fig. 1B).

To investigate eps8 tyrosine phosphorylation by the EGFR in a cell line which is physiologically responsive to EGF, we employed the BALB/MK cell line. These are mouse keratinocytes which are exquisitely sensitive to EGF (38). A Scatchard plot analysis of ^{125}I-labeled EGF binding to BALB/MK cells revealed around 1.5×10^4 EGF-binding sites with a single dissociation constant, on the order of 10^{-10} M (Table 1). Although BALB/MK cells express eps8 at an ~10-fold lower level than NIH-EGFR cells (Table 1), EGF stimulation readily induced its phosphorylation (Fig. 1C). On the basis of these results, we concluded that the *eps*8 product is phosphorylated in vivo under physiological conditions of activation of the EGFR kinase. It is not known whether eps8 is directly phosphorylated by EGFR. We want to point out, however, that we have shown direct physical interaction between eps8 and EGFR by a novel mechanism which is pTyr and SH2 independent (4). This finding makes the hypothesis of direct phosphorylation extremely likely.

Stoichiometry of phosphorylation of eps8 in vivo. We next estimated the percentage of eps8 molecules which is tyrosine phosphorylated in vivo following EGFR activation. To do this, we initially determined the optimal conditions for eps8 phosphorylation in vivo. EGF induced maximal eps8 phosphorylation at a concentration of 17 nM (Fig. 1 and data not shown); we therefore measured eps8 tyrosine phosphorylation following treatment of NIH-EGFR cells with 17 nM EGF as a function of time. As shown in Fig. 2A, eps8 phosphorylation was half maximal after 15 s of stimulation, reached a plateau at 1 min, and remained stable until 10 min of stimulation. Thus, we measured the stoichiometry of eps8 phosphorylation in vivo after 5 min of EGF treatment at a dose of 17 nM. To this end, cell lysates from EGF-treated NIH-EGFR were subjected to three sequential cycles of immunoprecipitation with anti-pTyr antibody followed by immunoblotting with an anti-eps8 antibody (Fig. 2B, top panel). Aliquots of the supernatant after the immunoprecipitations and of the total initial material were also analyzed in the immunoblot (Fig. 2B). After autoradiography, the signals were quantitated by phosphorimaging and the percentage of in vivo phosphorylation was calculated after correction for the amount of material loaded (see the legend to Fig. 2 and Materials and Methods for details). We estimated that ~30% of the total eps8 pool was phosphorylated under our conditions of analysis. In comparison, ezrin and PLC-γ showed tyrosine phosphorylation of ~10 and 3% of the total pool, respectively (Fig. 2B, middle and bottom panels, respectively).

The *eps*8 gene product is constitutively phosphorylated on tyrosine residues in human tumor cell lines. We next examined the state of phosphorylation of eps8 in a panel of human normal and tumor cell lines (listed in Table 2) under conditions of serum deprivation. As previously described, the human *eps*8 product was detected as a single species of 97 kDa and differences in the levels of expression of p97^{eps8} were detected, with cell lines of epithelial or mesodermal derivation displaying the highest levels (reference 43 and data not shown). Similar amounts of p97^{eps8} were immunoprecipitated with an anti-eps8 antibody and visualized with either an anti-pTyr or an anti-eps8 antibody (Fig. 3A). In several of the tumor cell lines, p97^{eps8} appeared to be constitutively tyrosine phosphorylated. Conversely, no tyrosine-phosphorylated p97^{eps8} was detected in normal cell lines (Fig. 3A and Table 2).

To estimate the percentage of p97^{eps8} molecules phosphorylated in the tumor cell lines, we followed the experimental protocol described in the legend to Fig. 2. The results of these experiments are shown in Fig. 3B for the 5637 bladder carcinoma cell line; similar results (not shown) were obtained with

TABLE 2. Tyrosine phosphorylation of RTK substrates in tumor-derived and normal cell lines[a]

Cell line	Derivation	Tyrosine phosphorylation				
		eps8	shc	PLC-γ	eps15	rasGAP
HOS	Osteosarcoma	+	−	−	−	−
HA1095	Synovial sarcoma	+	+	−	−	−
HT1080	Fibrosarcoma	+	+	−	−	−
Hep2	Larynx carcinoma	+	+	−	−	−
5637	Bladder carcinoma	+	+	−	−	−
A172	Astrocytoma	+	+	−	−	−
KG1	Acute myelocytic leukemia	±	+	+	−	−
HeLa	Cervix carcinoma	±	+	−	−	−
U937	Histiocytic lymphoma	±	+	−	−	−
SKBr3	Mammary adenocarcinoma	±	+	−	−	−
K562	Chronic myelocytic leukemia	−	+	−	−	−
HL60	Acute myelocytic leukemia	−	−	−	−	−
Calu1	Lung adenocarcinoma	−	−	−	−	−
MDAMB361	Mammary adenocarcinoma	−	−	−	−	−
A204	Rhabdomyosarcoma	−	−	−	−	−
M426	Normal fibroblasts	−	−	−	−	−
M413	Normal fibroblasts	−	−	−	−	−
AB589	Normal mammary cells	−	−	−	−	−

[a] The tumor-derived and normal cell lines indicated were serum starved for 24 h. Cellular proteins (3 to 5 mg) were immunoprecipitated with specific antibodies to the substrates and immunoblotted with anti-pTyr antibody. Results are expressed semiquantitatively as follows: +, strong signal; ±, weak signal; −, no signal. Refer to Fig. 3A and 5 for evaluation of the signals.

the HA1095 cell line. We estimated that around 3 to 5% of the total pool of p97^{eps8} (see the legend to Fig. 3B and Materials and Methods for details) is constitutively tyrosine phosphorylated in these cell lines.

Genetic alterations of tyrosine kinase pathways associated with constitutive eps8 phosphorylation in tumor cell lines. To identify pTyr-containing proteins physically associated with p97^{eps8} in tumor cell lines, we performed coimmunoprecipitation experiments. Total cellular proteins were extracted from HA1095 and 5637 cells under mild lysis conditions to preserve protein-protein interactions. Anti-eps8 immunoprecipitates were then immunoblotted with an anti-pTyr antibody. As shown in Fig. 4A, another pTyr-containing protein of ~180 kDa was detected, in addition to p97^{eps8}, in both cell lines. This protein was specifically coimmunoprecipitated with p97^{eps8}, as it was not detectable in immunoprecipitates obtained with preimmune control serum (Fig. 4A).

The 180-kDa protein might represent the kinase responsible for phosphorylation of p97^{eps8}, its molecular weight pointing to an RTK rather than to a nonreceptor tyrosine kinase. We therefore searched for constitutive tyrosine phosphorylation of several RTKs in HA1095 and 5637 cells, including EGFR, erbB-2/neu, erbB-3, erbB-4, and the platelet-derived growth

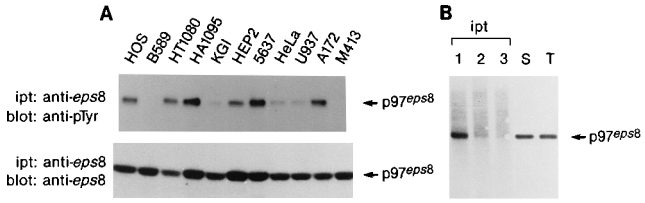

FIG. 3. Constitutive tyrosine phosphorylation of p97^{eps8} in human tumor cell lines. (A) Tyrosine phosphorylation. A selection of the analyzed cell lines is presented; a complete list of the cell lines analyzed is in Table 2. Cells were grown to confluence and then serum starved for 24 h in Dulbecco's modified Eagle's medium. Equal amounts of p97^{eps8} were immunoprecipitated with the anti-eps8 antibody, starting from different amounts of total cell lysates, on the basis of a preliminary characterization of the levels of p97^{eps8} present in the cells (data not shown). Detection was done with anti-pTyr (top panel) and anti-eps8 (bottom panel) antibodies. (B) Stoichiometry of p97^{eps8} phosphorylation in 5637 cells. Total cellular proteins (5 mg) from serum-starved 5637 cells were subjected to three cycles of immunoprecipitation with the anti-pTyr antibody as described in the legend to Fig. 2. Immunoprecipitates, the supernatant of the immunoprecipitation reaction (lane S, 1/50 of the total supernatant, corresponding to 100 μg of the initial material), and an aliquot of the total cellular proteins (lane T, 100 μg of proteins) were immunoblotted with the anti-eps8 antibody. Stoichiometry of phosphorylation was calculated as described in Materials and Methods. The position of eps8 is indicated.

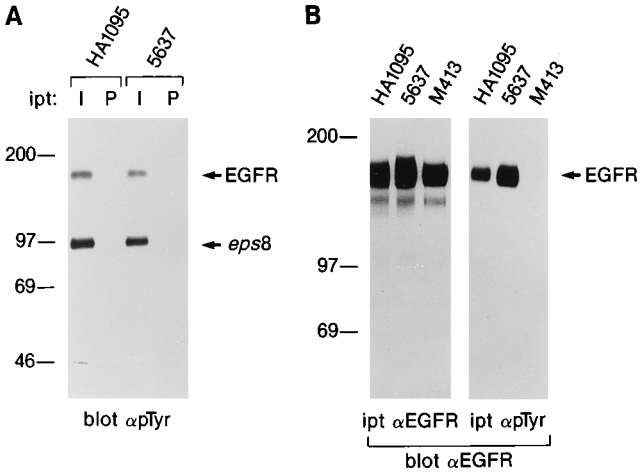

FIG. 4. Detection of a constitutively active EGFR in 5637 and HA1095 tumor cell lines. (A) Coimmunoprecipitations. Six milligrams of total cellular proteins, obtained under mild lysis conditions from the indicated cell lines depleted of serum for 24 h, was immunoprecipitated with the anti-eps8 antibody (I) or preimmune serum (P) and immunodetected with the anti-pTyr antibody. (B) Constitutive phosphorylation of EGFR. Two milligrams of total cellular proteins, from the indicated cell lines depleted of serum for 24 h, was immunoprecipitated with monoclonal antibody Ab-1 directed against the extracellular domain of the EGFR (left panel), or the anti-pTyr antibody (right panel). Immunoblotting was done with the E7 anti-EGFR peptide antibody. An experiment reciprocal to the one shown in the right panel (immunoprecipitation with anti-EGFR and blotting with anti-pTyr) yielded comparable results. Molecular size markers are shown in kilodaltons. The positions of EGFR and eps8 are also indicated.

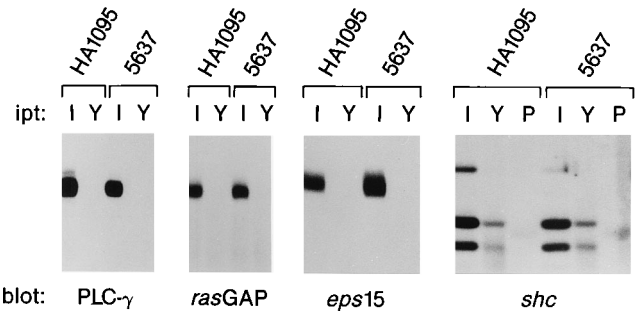

FIG. 5. Tyrosine phosphorylation of RTK substrates in the 5637 and HA1095 tumor cell lines. Total cellular proteins from the 5637 and HA1095 cell lines were immunoprecipitated with either substrate-specific sera (I), anti-pTyr antibody (Y), or preimmune serum (P). Immunoblots were detected with antibodies specific for the individual substrates (from left to right, anti-PLC-γ, anti-eps15, anti-rasGAP, and anti-shc). Comparable results were obtained in immunoprecipitations with specific antisubstrate antibodies followed by immunoblotting with anti-pTyr antibody (data not shown). The positions of individual RTK substrates are indicated.

TABLE 3. Transforming activity of eps8 cDNAs

Transfected DNA[a]	Transforming activity (FFU/pmol)[b]	
	Minus EGF	Plus EGF
LTR-meps8	$<10^0$	2×10^1
LTR-heps8	$<10^0$	2×10^1
LTR-EGFR	$<10^0$	3.5×10^2
LTR–PLC-γ	$<10^0$	$<10^0$
LTR control	$<10^0$	$<10^0$

[a] All of the eukaryotic expression constructs employed contained the gene of interest under the transcriptional control of the Moloney murine leukemia virus long terminal repeat (LTR) in either the pCEV (25) or the LTR-2 (7) vector. LTR-EGFR (6), LTR-meps8 (11), and LTR-heps8 (43) have already been described. LTR–PLC-γ was a kind gift of S. A. Aaronson.

[b] Transfection of NIH 3T3 cells was performed with 40 μg of calf thymus DNA as the carrier by the calcium phosphate precipitation technique (41). Where indicated, EGF (20 ng/ml) was added after 14 days. Focus-forming activity was scored at day 21 on duplicate plates transfected with serial tenfold dilutions of the DNAs of interest. Transforming activity is expressed in focus-forming units (FFU) per picomole of added DNA and is corrected for the efficiency of transfection calculated in parallel plates subjected to marker selection. Results are representative of three experiments performed in duplicate.

factor receptor. As shown in Fig. 4B, EGFR displayed constitutive tyrosine phosphorylation in serum-starved HA1095 and 5637 tumor cells, whereas it showed no detectable pTyr content in normal human M413 fibroblasts. None of the other RTKs analyzed displayed detectable constitutive pTyr content (data not shown). These results indicate that the EGFR-activated pathway is chronically activated in these tumor cell lines, resulting in steady-state tyrosine phosphorylation of p97^{eps8}.

It was of interest, therefore, to determine whether other known substrates of the EGFR were tyrosine phosphorylated in HA1095 and 5637 at steady state. We analyzed the pTyr content of shc, PLC-γ, rasGAP, and eps15 under conditions of serum starvation. As shown in Fig. 5, no pTyr-containing PLC-γ, rasGAP, or eps15 was detected; shc, however, was constitutively tyrosine phosphorylated in both cell lines. Simultaneous tyrosine phosphorylation of shc and eps8 correlated well in several other tumor cell lines (Table 2). Conversely, with the exception of PLC-γ in KG1 cells, no constitutive pTyr content was detectable in PLC-γ, rasGAP, and eps15. It is noteworthy that in most lines of hematopoietic origin, eps8 tyrosine phosphorylation was not detectable, whereas shc constitutively displayed pTyr (reference 28 and data not shown). It is possible that our inability to detect pTyr-containing eps8 is due to the low levels of eps8 expression in hematopoietic cells (43). Alternatively, the group of tumors with eps8 phosphorylation might represent a subset of those displaying shc phosphorylation. Whatever the case, constitutive tyrosine phosphorylation, in cell lines with genetic alterations of the EGFR pathway, is a property shared in several cases by eps8 and shc but cannot be generalized for other second messengers.

Overexpression of eps8 induces EGF-dependent transformation of NIH 3T3 cells. Constitutive tyrosine phosphorylation of eps8 in tumor cell lines with a chronically active EGFR pathway(s) might be relevant to the transformed state of these cells. If so, increased eps8 phosphorylation under rate-limiting conditions of EGFR signaling might confer a proliferative advantage and possibly result in malignant transformation in a model system.

NIH 3T3 cells harbor low levels of EGFR ($\sim 5 \times 10^3$ receptors per cell). EGF, in combination with insulin, is sufficient to sustain proliferation but is not sufficient to induce the appearance of transformed foci (6). Nevertheless, NIH 3T3 cells are susceptible to EGFR-mediated transformation, which can be achieved by overexpression of EGFR and ligand stimulation (6). We therefore transfected into NIH 3T3 cells two eukaryotic expression vectors encoding the mouse or human eps8 open reading frame (LTR-meps8 [11] and LTR-heps8 [43]). As shown in Table 3, neither vector induced transformation in the absence of EGF. Addition of EGF to the culture medium, however, resulted in the appearance of transformed foci with an efficiency ~20-fold lower than that obtained by transfection of the EGFR (Table 3). In comparison, a PLC-γ expression vector did not induce transformation in the absence or in the presence of EGF treatment (Table 3).

Physical interaction between eps8 and shc. To gain insight into the function of eps8, we investigated its interaction with shc, since both proteins are constitutively phosphorylated in human tumor cell lines. We initially determined physical association in vivo in NIH-EGFR cells by performing coimmunoprecipitations. As shown in Fig. 6, shc was recovered from anti-eps8 immunoprecipitates and vice versa. Of note, only a minor fraction of the total cellular shc and eps8 (~0.3%, from our calculations) coimmunoprecipitated (Fig. 6). This could be due to instability of the complex under our condition of lysis. It may also reflect an in vivo situation in which shc and eps8 are individually involved in multiple interactions, with only a fraction of the respective pools available for the formation of an shc-eps8 complex. This possibility is supported by findings that the eps8 SH3 domain mediates multiple interactions. Although eps8 could not be coimmunoprecipitated with any of the other substrates analyzed in this study, namely, PLC-γ, rasGAP, ezrin, and eps15 (data not shown), it interacts, through its SH3 domain, with shb (21) and several other proteins (42).

The association between shc and eps8 was comparable in serum-starved cells and EGF-treated cells (Fig. 6). In serum-starved cells, both eps8 and shc display little, if any, tyrosine phosphorylation, whereas under the conditions of EGF treatment employed in our study, they showed a more than 20-fold increase in tyrosine phosphorylation and were phosphorylated at high stoichiometry (data not shown, Fig. 1 and 2, and references 11 and 27). Thus, the interaction between eps8 and shc is not likely to involve the SH2 or PTB (22) domain of shc and pTyr of eps8, since it is pTyr independent. eps8, however, possesses an SH3 domain which might bind one of several proline-rich regions present in shc. We decided to test this possibility by in vitro binding experiments.

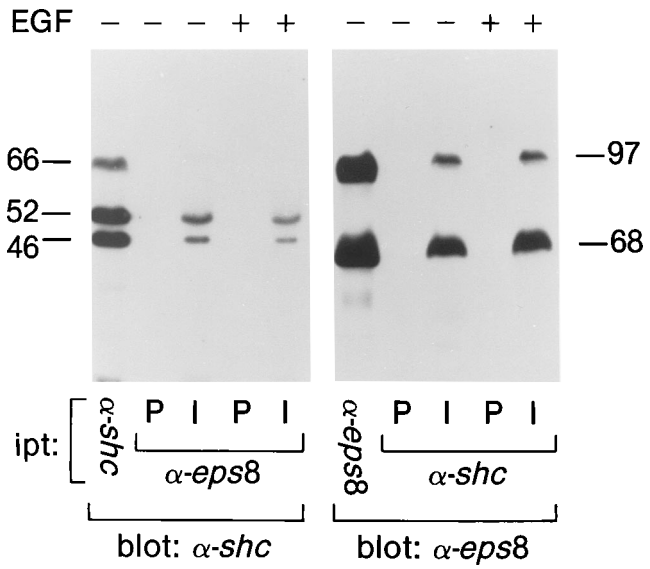

FIG. 6. Coimmunoprecipitation of eps8 and shc in vivo. NIH-EGFR cells were serum starved for 24 h and then treated with EGF (17 nM, at 37°C for 10 min, + lanes) or mock treated (− lanes). Twelve milligrams of total cellular proteins, obtained under mild lysis conditions to preserve protein-protein interactions, was immunoprecipitated with either anti-shc or anti-eps8 serum (I) or preimmune serum (P) and blotted with anti-shc or anti-eps8 serum. The left panel shows immunoprecipitation with anti-eps8 and blotting with anti-shc, and the right panel shows immunoprecipitation with anti-shc and blotting with anti-eps8. The first lane in both panels is an immunoprecipitation (0.2 mg of total lysates), followed by immunoblotting with the same antibody (anti-shc–anti-shc in the left panel and anti-eps8–anti-eps8 in the right panel), as a reference. The positions of the shc and eps8 products are indicated, and their respective molecular masses are given in kilodaltons.

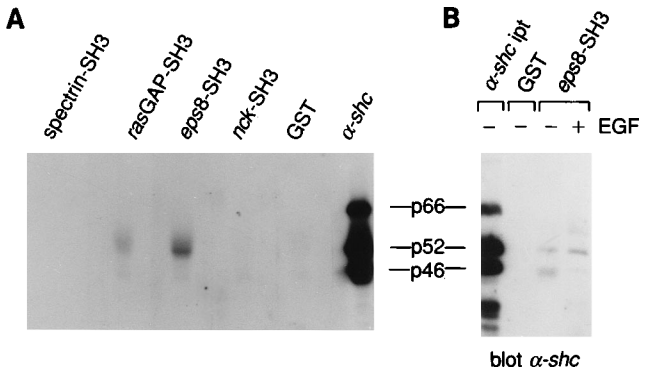

FIG. 7. In vitro interaction between shc and the SH3 domain of eps8. (A) Far Western blotting. Two milligrams of total cellular proteins from serum-starved NIH-EGFR cells was immunoprecipitated with an anti-shc antibody and blotted following sodium dodecyl sulfate-polyacrylamide gel electrophoresis. Blots were incubated with GST–eps8-SH3, GST–nck-SH3, GST–rasGAP-SH3, GST–spectrin-SH3, or GST, and detection was done with an affinity-purified anti-GST antibody, as indicated in Materials and Methods. The last lane was immunodetected with an anti-shc antibody for comparison. (B) In vitro binding. GST–eps8-SH3 and control GST were immobilized on agarose-conjugated glutathione and then incubated with total cellular proteins from serum-starved (lanes −) or EGF-treated (lane +) NIH-EGFR cells. Specifically bound material was analyzed by sodium dodecyl sulfate-polyacrylamide gel electrophoresis followed by immunoblotting with an anti-shc antibody. The first lane is an immunoprecipitate with anti-shc blotted with anti-shc as a reference. The positions of the shc products are indicated.

In a first series of experiments, we immunoprecipitated shc from total cellular proteins and analyzed its ability to bind to the eps8 SH3 domain and other SH3 domains in a far Western assay. As shown in Fig. 7A, the SH3 domain of eps8 fused to GST (GST–eps8-SH3) interacted with shc, while control GST was unable to do so. A fusion protein containing the first SH3 domain of nck (GST–nck-SH3), which displays the highest sequence similarity to the eps8 SH3 domain (11), and a GST–spectrin-SH3 fusion also exhibited little, if any, in vitro association with shc (Fig. 7A). The SH3-binding ability of shc was, however, not restricted to eps8, since a GST–rasGAP-SH3 fusion also recognized the immunoprecipitated shc (Fig. 7A). In addition, shc has been shown to be recoverable from total cellular proteins by immobilized SH3 domains from src, fyn, and lyn (40).

We finally tested whether native shc could be recognized by the eps8 SH3 domain. As shown in Fig. 7B, immobilized GST–eps8-SH3, but not immobilized GST, was able to recover shc proteins from total cellular lysates. While p52shc was detectable in both types of in vitro binding, p46shc was easily recoverable from total cellular lysates by immobilized GST–eps8-SH3 (Fig. 7B) but less well detected in a far Western blot (Fig. 7A). There is no immediate explanation for this finding. In addition, we did not manage to detect binding of the eps8 SH3 domain to p66shc, possibly because of the lower abundance of this shc isoform. Whatever the case, the sum of our results indicates that the physical association between eps8 and shc is mediated, at least in part, by the SH3 domain of eps8.

DISCUSSION

Evidence of a role of eps8 in mitogenicity originates from the observation that its overexpression enhances the EGF responsiveness of different cell types (11). The findings of the present study establish eps8 as a physiological EGFR substrate. In the NIH-EGFR model system, tyrosine phosphorylation of eps8 was detected under rate-limiting conditions of EGF triggering. Furthermore, the dose-response kinetic of eps8 phosphorylation resembled that of PLC-γ, a previously established EGFR substrate that has also been implicated in EGF-dependent mitogenicity (37). The sum of these observations provides strong support for the notion that eps8 is physiologically involved in the transduction of EGF-activated mitogenic signals.

Constitutive tyrosine phosphorylation of p97^{eps8} in several tumor cell lines indicated a role for eps8 in neoplastic growth. In two representative cell lines, HA1095 and 5637, initial detection of phosphorylated eps8 led to the finding of constitutively active EGFRs. It is not known whether activation of EGFR in these cells is due to the existence of autocrine loops or to intrinsic receptor alterations. Whatever the case, detection of pTyr-containing eps8 appears to be a useful marker of lesions affecting tyrosine kinase-activated pathways in tumor cells. Phosphorylation of eps8 in tumor cell lines was detected at levels which are associated with potent mitogenic response in a model system. We calculated that ~4% of the eps8 pool was constitutively phosphorylated on tyrosine in HA1095 and 5637 tumor cells. In the NIH-EGFR model system, 30% of the total eps8 contained pTyr under maximal EGF stimulation. We estimated that at the half-maximal EGF dose, 3 to 4% of the total pool would be phosphorylated (10% of the maximal level; Fig. 1), a value in agreement with that detected in tumor cell lines. This strongly suggests that constitutive tyrosine phosphorylation of eps8 in tumor cells has functional implications for proliferation.

This possibility is further strengthened by our finding that transfection of eps8 expression vectors confers a conditional

EGF-dependent transformed phenotype on NIH 3T3 cells. This result is consistent with the possibility that under rate-limiting conditions of activation of the EGFR pathway, overexpression of eps8 facilitates its phosphorylation. Tyrosine phosphorylation of eps8 above a critical threshold might, in turn, result in enhanced downstream signaling and a proliferative advantage.

Among various substrates analyzed in tumor cell lines, the propensity for constitutive phosphorylation of eps8 and shc was striking. An obvious explanation for this phenomenon is that some tumor cell lines harbor activated tyrosine kinases that preferentially phosphorylate eps8 and shc. However, on the basis of the finding of a chronically active EGFR in HA1095 and 5637, additional mechanisms might be responsible, since the EGFR can efficiently phosphorylate all of the substrates analyzed (for reviews, see references 18, 31, and 32 and references therein). Preferential phosphorylation of eps8 and shc, as opposed to PLC-γ, rasGAP, and eps15, may be selected in some tumor cell lines because of their ability to confer a growth advantage. Although the molecular mechanisms responsible for this phenomenon are not known, tyrosine phosphorylation of intracellular transducers is tightly controlled by the activity of tyrosine phosphatases (19, 35, 36, and references therein). These enzymes possess different degrees of specificity towards individual substrates. Thus, one can speculate that alterations in the balance of kinase and specific phosphatase activity for eps8 and shc might result in constitutive tyrosine phosphorylation and downstream signaling in some tumor cell lines.

Possible cooperation between eps8 and shc was further substantiated by the finding of their physical association in vivo. This was demonstrated by coimmunoprecipitation experiments and could also be correlated with colocalization in the perinuclear area of a fraction of the eps8 and shc pools (data not shown). Interaction between eps8 and shc does not depend on pTyr-SH2 interactions because it occurs in a pTyr-independent manner. Conversely, we showed that it is mediated, at least in part, by the SH3 domain of eps8. Evidence indicating that the binding abilities of shc do not depend solely on its SH2 domain is indeed accumulating. Habib et al. showed an association between the PEST tyrosine phosphatase (PTP-PEST) and shc (17) and suggested that the initial 45 amino acids of the p52shc isoform contain the binding site for PTP-PEST. In addition, recent evidence has pointed to the existence of an atypical SH2-like domain in the N-terminal region of shc (22). Finally, various SH3 domains can recognize shc in in vitro binding assays (40).

In eps8 and shc, the shc binding interface for the eps8 SH3 domain is likely to localize to the collagen homology region, which contains several proline-rich stretches that might function as SH3-binding sites (27). Another adapter molecule, shb (39), also binds to the SH3 domain of eps8 (21). Structural similarities between shc and shb include a C-terminal SH2 domain and proline-rich regions upstream. They might, therefore, identify a subfamily of evolutionarily convergent transducers with pTyr- and SH3-binding abilities which bind to eps8. In this regard, it has been noted that two of five proline-rich regions of shb (PPPGPGR and RPSQPPQAVPQA) display good homology with shc regions 303 to 309 and 359 to 370, respectively, thus possibly representing eps8-binding sites.

The function of an eps8-shc complex in the signaling pathway is not known. An attractive possibility is suggested by our recent finding that the isolated SH3 domain of eps8 is capable of inducing maturation of *Xenopus* oocytes and is likely to act upstream of ras in this system (42). One can then speculate that an eps8-shc complex might be involved in the activation of ras, a possibility that warrants further investigation.

It is conceivable that eps8 functions at multiple points in the signaling cascade. The predicted structure of eps8 revealed the presence of several possible binding domains, including an SH3 domain, a nuclear targeting sequence, and a split putative PH domain (11, 43). Its tyrosine phosphorylation might determine SH2-binding abilities as well. Furthermore, we have demonstrated the presence in eps8 of a novel binding domain capable of binding to the juxtamembrane region of the EGFR with a mechanism which is pTyr and SH2 independent (4). Taken together, these observations indicate extensive networking abilities of eps8. At the cellular level, this appears to correlate with multiple localizations of eps8, as detected by immunofluorescence (2). We are presently cloning intracellular proteins associating with the SH3 and PH domains of eps8 to characterize the entire repertoire of eps8-binding molecules. Molecular characterization of these molecules should provide a better understanding of the role of eps8 in signaling and of its subversions in the neoplastic process.

REFERENCES

1. **Birge, R. B., and H. Hanafusa.** 1993. Closing in on SH2 specificity. Science **262:**1522–1524.
2. **Carbone, R., W. T. Wong, and P. P. Di Fiore.** Unpublished observations.
3. **Carpenter, G.** 1992. Receptor tyrosine kinase substrates: src homology domains and signal transduction. FASEB J. **6:**3283–3289.
4. **Castagnino, P., Z. Biesova, W. T. Wong, F. Fazioli, G. N. Gill, and P. P. Di Fiore.** 1995. Direct binding of *eps*8 to the juxtamembrane domain of EGFR is phosphotyrosine- and SH2-independent. Oncogene **10:**723–729.
5. **Cicchetti, P., B. J. Mayer, G. Thiel, and D. Baltimore.** 1992. Identification of a protein that binds to the SH3 region of Abl and is similar to Bcr and GAP-rho. Science **257:**803–806.
6. **Di Fiore, P. P., J. H. Pierce, T. P. Fleming, R. Hazan, A. Ullrich, C. R. King, J. Schlessinger, and S. A. Aaronson.** 1987. Overexpression of the human EGF receptor confers an EGF-dependent transformed phenotype to NIH 3T3 cells. Cell **51:**1063–1070.
7. **Di Fiore, P. P., J. H. Pierce, M. H. Kraus, O. Segatto, C. R. King, and S. A. Aaronson.** 1987. erbB-2 is a potent oncogene when overexpressed in NIH/3T3 cells. Science **237:**178–182.
8. **Di Fiore, P. P., O. Segatto, F. Lonardo, F. Fazioli, J. H. Pierce, and S. A. Aaronson.** 1990. The carboxy-terminal domains of *erbB-2* and epidermal growth factor receptor exert different regulatory effects on intrinsic receptor tyrosine kinase function and transforming activity. Mol. Cell. Biol. **10:**2749–2756.
9. **Fantl, W. J., D. E. Johnson, and L. T. Williams.** 1993. Signaling by receptor tyrosine kinases. Annu. Rev. Biochem. **62:**453–481.
10. **Fazioli, F., D. P. Bottaro, L. Minichiello, A. Auricchio, W. T. Wong, O. Segatto, and P. P. Di Fiore.** 1992. Identification and biochemical characterization of novel putative substrates for the epidermal growth factor receptor kinase. J. Biol. Chem. **267:**5155–5161.
11. **Fazioli, F., L. Minichiello, V. Matoska, P. Castagnino, T. Miki, W. T. Wong, and P. P. Di Fiore.** 1993. Eps8, a substrate for the epidermal growth factor receptor kinase, enhances EGF-dependent mitogenic signals. EMBO J. **12:**3799–3808.
12. **Fazioli, F., L. Minichiello, B. Matoškovā, W. T. Wong, and P. P. Di Fiore.** 1993. eps15, a novel tyrosine kinase substrate, exhibits transforming activity. Mol. Cell. Biol. **13:**5814–5828.
13. **Fazioli, F., W. T. Wong, S. J. Ullrich, K. Sakaguchi, E. Appella, and P. P. Di Fiore.** 1993. The ezrin-like family of tyrosine kinase substrates: receptor-specific pattern of tyrosine phosphorylation and relationship to malignant transformation. Oncogene **8:**1335–1345.
14. **Gibson, T. J., M. Hyvonen, A. Musacchio, M. Saraste, and E. Birney.** 1994. PH domain: the first anniversary. Trends Biochem. Sci. **19:**349–353.
15. **Glenney, J. R.** 1991. Isolation of tyrosine-phosphorylated proteins and generation of monoclonal antibodies. Methods Enzymol. **201:**92–100.
16. **Gout, I., R. Dhand, I. D. Hiles, M. J. Fry, G. Panayotou, P. Das, O. Truong, N. F. Totty, J. Hsuan, and G. W. Booker.** 1993. The GTPase dynamin binds to and is activated by a subset of SH3 domains. Cell **75:**25–36.
17. **Habib, T., R. Herrera, and S. J. Decker.** 1994. Activators of protein kinase C stimulate association of Shc and the PEST tyrosine phosphatase. J. Biol. Chem. **269:**25243–25246.
18. **Hernandez-Sotomayor, S. M., and G. Carpenter.** 1992. Epidermal growth factor receptor: elements of intracellular communication. J. Membr. Biol. **128:**81–89.
19. **Hunter, T., R. A. Lindberg, D. S. Middlemas, S. Tracy, and P. van der Geer.** 1992. Receptor protein tyrosine kinases and phosphatases. Cold Spring Har-

bor Symp. Quant. Biol. **57:**25–42.
20. **Kanner, S. B., A. B. Reynolds, R. R. Vines, and J. T. Parsons.** 1990. Monoclonal antibodies to individual tyrosine-phosphorylated protein substrates of oncogene-encoded tyrosine kinases. Proc. Natl. Acad. Sci. USA **87:**3328–3332.
21. **Karlsson, T., Z. Songyang, E. Landgren, C. Lavergne, P. P. Di Fiore, M. Anafi, T. Pawson, L. C. Cantley, L. Claesson-Welsh, and M. Welsh.** Molecular interactions of the src homology 2 domain protein shb with phosphotyrosine residues, tyrosine kinase receptors and src homology 3 domain proteins. Oncogene, in press.
22. **Kavanaugh, W. M., and L. T. Williams.** 1994. An alternative to SH2 domains for binding tyrosine-phosphorylated proteins. Science **266:**1862–1865.
23. **Kazlauskas, A.** 1994. Receptor tyrosine kinases and their targets. Curr. Opin. Genet. Dev. **4:**5–14.
24. **Lowenstein, E. J., R. J. Daly, A. G. Batzer, W. Li, B. Margolis, R. Lammers, A. Ullrich, E. Y. Skolnik, D. Bar-Sagi, and J. Schlessinger.** 1992. The SH2 and SH3 domain-containing protein GRB2 links receptor tyrosine kinases to ras signaling. Cell **70:**431–442.
25. **Miki, T., T. P. Fleming, D. P. Bottaro, J. S. Rubin, D. Ron, and S. A. Aaronson.** 1991. Expression cDNA cloning of the KGF receptor by creation of a transforming autocrine loop. Science **251:**72–75.
26. **Munson, P. J., and D. Rodbard.** 1980. Ligand: a versatile computerized approach for characterization of ligand-binding systems. Anal. Biochem. **107:**220–239.
27. **Pelicci, G., L. Lanfrancone, F. Grignani, J. McGlade, F. Cavallo, G. Forni, I. Nicoletti, T. Pawson, and P. G. Pelicci.** 1992. A novel transforming protein (SHC) with an SH2 domain is implicated in mitogenic signal transduction. Cell **70:**93–104.
28. **Pelicci, G., L. Lanfrancone, A. E. Salcini, A. Romano, S. Mele, M. G. Borrello, O. Segatto, P. P. Di Fiore, and P. G. Pelicci.** Constitutive phosphorylation of shc proteins in human tumors. Submitted for publication.
29. **Ren, R., B. J. Mayer, P. Cicchetti, and D. Baltimore.** 1993. Identification of a ten-amino acid proline-rich SH3 binding site. Science **259:**1157–1161.
30. **Romano, A., W. T. Wong, M. Santoro, P. J. Wirth, S. S. Thorgeirsson, and P. P. Di Fiore.** 1994. The high transforming potency of erbB-2 and ret is associated with phosphorylation of paxillin and a 23 kDa protein. Oncogene **9:**2923–2933.
31. **Schlessinger, J.** 1994. SH2/SH3 signaling proteins. Curr. Opin. Genet. Dev. **4:**25–30.
32. **Schlessinger, J., and A. Ullrich.** 1992. Growth factor signaling by receptor tyrosine kinases. Neuron **9:**383–391.
33. **Skolnik, E. Y., B. Margolis, M. Mohammadi, E. Lowenstein, R. Fischer, A. Drepps, A. Ullrich, and J. Schlessinger.** 1991. Cloning of PI3 kinase-associated p85 utilizing a novel method for expression/cloning of target proteins for receptor tyrosine kinases. Cell **65:**83–90.
34. **Songyang, Z., S. E. Shoelson, M. Chaudhuri, G. Gish, T. Pawson, W. G. Haser, F. King, T. Roberts, S. Ratnofsky, and R. J. Lechleider.** 1993. SH2 domains recognize specific phosphopeptide sequences. Cell **72:**767–778.
35. **Tonks, N. K., A. J. Flint, M. F. Gebbink, H. Sun, and Q. Yang.** 1993. Signal transduction and protein tyrosine dephosphorylation. Adv. Second Messenger Phosphoprotein Res. **28:**203–210.
36. **Tonks, N. K., Q. Yang, A. J. Flint, M. F. Gebbink, B. R. Franza, Jr., D. E. Hill, and S. Brady-Kalnay.** 1992. Protein tyrosine phosphatases: the problem of a growing family. Cold Spring Harbor Symp. Quant. Biol. **57:**87–94.
37. **Valius, M., and A. Kazlauskas.** 1993. Phospholipase C-gamma 1 and phosphatidylinositol 3 kinase are the downstream mediators of the PDGF receptor's mitogenic signal. Cell **73:**321–334.
38. **Weissman, B. E., and S. A. Aaronson.** 1983. BALB and Kirsten murine sarcoma viruses alter growth and differentiation of EGF-dependent balb/c mouse epidermal keratinocyte lines. Cell **32:**599–606.
39. **Welsh, M., J. Mares, T. Karlsson, C. Lavergne, B. Breant, and L. Claesson-Welsh.** 1994. Shb is a ubiquitously expressed Src homology 2 protein. Oncogene **9:**19–27.
40. **Weng, Z., S. M. Thomas, R. J. Rickles, J. A. Taylor, A. W. Brauer, C. Seidel-Dugan, W. M. Michael, G. Dreyfuss, and J. S. Brugge.** 1994. Identification of Src, Fyn, and Lyn SH3-binding proteins: implications for a function of SH3 domains. Mol. Cell. Biol. **14:**4509–4521.
41. **Wigler, M., S. Silverstein, L. S. Lee, A. Pellicer, Y. Cheng, and R. Axel.** 1977. Transfer of purified herpes virus thymidine kinase gene to cultured mouse cells. Cell **11:**223–232.
42. **Wong, W. T., P. Aroca, E. Santos, and P. P. Di Fiore.** Unpublished observations.
43. **Wong, W. T., F. Carlomagno, T. Druck, C. Barletta, C. M. Croce, K. Huebner, M. H. Kraus, and P. P. Di Fiore.** 1994. Evolutionary conservation of the EPS8 gene and its mapping to human chromosome 12q23-q24. Oncogene **9:**3057–3061.
44. **Yu, H., J. K. Chen, S. Feng, D. C. Dalgarno, A. W. Brauer, and S. L. Schreiber.** 1994. Structural basis for the binding of proline-rich peptides to SH3 domains. Cell **76:**933–945.